Polymer Chemistry

PAPER

View Article Online
View Journal | View Issue

Cite this: *Polym. Chem.*, 2018, **9**, 2271

An L-proline based thermoresponsive and pH-switchable nanogel as a drug delivery vehicle†

Y. Salinas, A. M. Castilla and M. Resmini *

The synthesis and characterisation of a novel dual stimuli-responsive nanogel, based on thermoresponsive *N*-*n*-propylacrylamide and an L-proline based monomer acting as a pH-switcher, is reported here. The effect of the crosslinker/co-monomer ratios was studied to demonstrate the relationship between the chemical structure, degree of hydrophobicity and physico-chemical characteristics of the nanogels. Tailoring of the thermoresponsive properties was achieved by altering crosslinker *N*,*N*′-methylenebis (acrylamide) content between 10 and 50 mol%, in combination with three thermoresponsive monomers *N*-*n*-isopropylacrylamide, *N*-*n*-propylacrylamide and *N*-acryloylpyrrolidine. A library of 25 different combinations of monomers and crosslinkers was obtained and characterised by dynamic light scattering and UV-Vis spectroscopy. The nanogel based on *N*-*n*-propylacrylamide and 10 mol% crosslinker was then co-polymerised with an L-proline based monomer to introduce a pH-switch. This nanogel was obtained with <10 nm particle size and a VPTT *ca.* 43 °C, and was used to demonstrate a drug delivery capability using Nile Blue A as a model drug. Detailed studies demonstrated maximum drug release at lower pH and 43 °C, thus confirming the dual stimuli switch.

Received 22nd February 2018,
Accepted 24th March 2018

DOI: 10.1039/c8py00308d

rsc.li/polymers

Introduction

'Smart' polymers constitute a growing area of research, due to their great potential for use as delivery systems.[1–3] Conventional approaches have shown the limitations of untriggered release, where Fickian diffusion drives non-specific cargo delivery.[4] A variety of intelligent materials have been engineered to respond to stimuli such as pH,[5] temperature,[6] light[7] and magnetic field,[8] with temperature being the most studied.[9] Thermoresponsive polymers undergo conformational changes at a specific temperature, known as the lower critical solution temperature (LCST). This often results in variations in their physico-chemical characteristics, such as size, shape and solubility. Following the first report on thermoresponsive liposomes,[10] considerable work has been done in the area of stimuli-responsive polymers. The applications of these systems have been developed in areas such as drug and gene delivery,[11,12] tissue engineering,[13] detection and sensing.[14] More recently, research has focused on materials with dual functionality, where two stimuli are combined.[15] In particular, materials showing dual temperature and pH response characteristics have been developed for drug delivery applications,[16] demonstrating efficient tailored release.[17,18]

The area of stimuli-triggered drug delivery has witnessed significant advances, with systems such as polymersomes,[19] dendrimers[20] and nanocomposite hydrogels[21] all showing promising results. Among the different matrices, polymeric nanogels have been widely investigated[22] since they were first reported in 1935,[23] owing to their cargo-releasing applications.[24] The swelling properties in water and the stability of the crosslinked matrix are key features that offer advantages in terms of cargo loading capacity, compared to self-assembled systems.[25] These are complemented by the formation of stable colloidal solutions and the possibility of tailoring their physico-chemical properties by changing the chemical composition.

N-Isopropylacrylamide (NIPAM)-based hydrogels have been extensively studied, since they show a volume phase transition temperature (VPTT) close to body temperature.[26,27] In addition, in recent years, a number of different monomers showing thermoresponsive properties have been explored with the aim of increasing the range of temperatures in which these materials can operate and thus the number of different applications.[28] Where dual functionalities have been investigated, the approach has commonly involved the introduction of pH responsive monomers, such as acrylic acid (AAc), methacrylic

Department of Chemistry and Biochemistry, SBCS, Queen Mary University of London, Mile End Road E1 4NS, London, UK. E-mail: m.resmini@qmul.ac.uk; Fax: +44 (0)2078827427; Tel: +44 (0)2078828054

†Electronic supplementary information (ESI) available: Chemical composition for the preparation of nanogels **N1–N31**; results of NMR analyses for polymerisations **N1–N30**; transmittance changes with temperature for nanogels **N1–N31** and transmittance changes with heating and cooling cycles for nanogels **N1**, **N6** and **N11**; FT-IR spectra of monomers NIPAM, NPAM, NAPr and A-Pro-OH, and nanogels **N1**, **N6** and **N11**; raw DLS data for nanogels **N1–32**; zeta potential for nanogels **N26–31**; NBA calibration curve. See DOI: 10.1039/c8py00308d

acid or 4-vinylpyridine.[29–32] Despite significant advances, the relationship between the chemical composition of the polymerisation mixtures and the properties of the materials is yet to be fully understood. This significantly limits the development of further applications.

In this work, we prepared a small library of nanogels, using three thermoresponsive monomers in combination with varying percentages of *N,N′*-methylenebis(acrylamide) (MBA) as a crosslinker, to study the impact of chemical composition on their morphology and thermoresponsive properties. We then introduced a pH-switch into the matrix, by using a novel polymerisable proline-derivative, to develop dual temperature/pH responsive materials. We selected one of the formulations to demonstrate the potential application of the new nanogels as drug-delivery vehicles. The presence of the carboxylic group enhances the efficient encapsulation *via* ionic interactions, allowing tailored release in different pH environments.

Experimental section

Materials

N-Isopropylacrylamide (NIPAM) (Aldrich, 97%), acryloyl chloride (Alfa Aesar, 96%, 400 ppm phenothiazine stabilizer), *N,N′*-methylenebis(acrylamide) (MBA) (Aldrich, 99%), propylamine (Aldrich, 98%), acrylic acid (AAc) (Aldrich, 200 ppm MEHQ as an inhibitor, 99%), L-proline ReagentPlus (Aldrich, ≥99%), pyrrolidine (Fluka, puriss. p.a., ≥99.0%), potassium hydroxide (laboratory reagent grade, Fisher Chemical), triethylamine (Aldrich, ≥99.5%), Nile Blue A (Alfa Aesar), and 1,2,4,5-tetramethylbenzene (Aldrich) were used as received. 2,2′-Azobisisobutyronitrile (AIBN) (Aldrich, 98%) was used after recrystallisation in methanol. All solvents were used as received. The dialysis membrane (MWCO 3500 Da, width 34 mm, diameter 22 mm) was purchased from Medicell International Ltd. Deuterated solvents were purchased from Goss Scientific and used without any further purification.

Characterisation studies

^{1}H and ^{13}C NMR spectra were recorded at 298 K using Bruker AV 400 MHz BBO Probe and AVIII 400 MHz BBO Probe spectrometers. Chemical shifts for ^{1}H and ^{13}C are reported in parts per million (δ); δ_H values are referenced to the residual solvent signal of $CDCl_3$ and DMSO-d_6 at δ = 7.26 ppm and 2.50, ppm, respectively. δ_C values are referenced to the solvent signal of $CDCl_3$ and DMSO-d_6 at δ = 77.16 and 39.52 ppm, respectively. NMR signals are reported in terms of chemical shifts (δ) in ppm, multiplicity, coupling constant (J) in hertz (Hz), relative integral and assignment, in that order. Spectra were processed using Bruker Topspin 4.0.1. 1,2,4,5-Tetramethylbenzene was used as an internal standard (δ = 6.9, 2.1 ppm) for the quantification of ^{1}H NMR experiments. Infrared spectra were recorded on a PerkinElmer Spectrum 65 FT-IR spectrometer equipped with a universal ATR sampling accessory. Nanogel hydrodynamic diameter (d_h) and zeta potential (ζ) measurements were performed by dynamic light scattering (DLS) with a Zetasizer Nano ZS (Malvern Instruments Ltd, UK) at 25 °C. All measurements were performed in triplicate (at a concentration of 1 mg mL^{-1}) after filtering through a 0.2 μm syringe filter. Transmission Electron Microscopy (TEM) images were captured using a JEOL JEM-1230 at 80 kV. A drop of a 1 mg mL^{-1} solution of the nanogel particles in water was placed onto a 300 Mesh Cu grid coated with carbon (Agar Scientific) and dried overnight. Volume phase transition temperatures (VPTT) were determined by monitoring the optical transmittance at 500 nm of the nanogels in deionised water (1 mg mL^{-1}), at temperatures ranging from 23 °C to 80 °C (1 °C min^{-1}), using a PerkinElmer Lambda 35 UV-Visible spectrometer equipped with a Peltier temperature programmer PTP$_{-1}^{+1}$. The VPTT was determined at the sudden slope change in the transmittance curve (50% transmittance value). Fluorescence studies were carried out with a FluoroMax-3 (Horiba Jobin Yvon) spectrophotometer.

Synthesis of monomer *N*-*n*-propylacrylamide (NPAM)

The synthesis was conducted according to a procedure reported in the literature with slight modifications.[33] Acryloyl chloride (1.53 g, 17 mmol) was dissolved in toluene (50 mL) and stirred under a N_2 atmosphere at −78 °C (using an acetone-dry ice bath). *N*-Propylamine (2 g, 34 mmol) was added dropwise to the solution for 30 min. The reaction mixture was kept in a freezer for 12 h. The white precipitate (*N*-propylamine hydrochloride salt) formed was filtered off. The resulting solution was concentrated by rotary-evaporation to yield pure NPAM monomer as a colourless oil (1.40 g, yield: 73%). ^{1}H NMR (400 MHz, $CDCl_3$): δ = 0.94 (t, J = 7.4 Hz, 3H, NH–CH_2–CH_2–C***H*****$_3$**), 1.56 (q, J = 7.4 Hz, 2H, NH–CH_2–C***H*****$_2$**–), 3.30 (app dt, J = 7.1, 4.9 Hz, 2H, NH–C***H*****$_2$**–), 5.63 (m, J = 10.1, 1.6 Hz, 1H, C***H*****$_2$**=CH–), 6.08 (dd, J = 17.0, 10.2 Hz, 1H, CH_2=C***H***–), 6.27 (dd, J = 16.8, 1.6 Hz, 1H, C***H*****$_2$**=CH–); ^{13}C NMR (101 MHz, $CDCl_3$): δ = 11.37 (NH–CH_2–CH_2–***C***H_3), 22.75 (NH–CH_2–***C***H_2), 41.33 (NH–***C***H_2), 126.00 (***C***H_2=CH), 131.05 (CH_2=***C***H), 165.79 (***C***=O).

Synthesis of monomer *N*-acryloylpyrrolidine (NAPr)

The synthesis was conducted according to a procedure reported in the literature with slight modifications.[34] Pyrrolidine (3.56 g, 50 mmol) and triethylamine (5.56 g, 55 mmol) were dissolved in dichloromethane (100 mL) under N_2 at −78 °C (using an acetone-dry ice bath). To the reaction solution was added dropwise acryloyl chloride (5.43 g, 60 mmol) over 30 min and the reaction was stirred for 1 h at 0 °C, followed by 2 h at room temperature. The solution was then washed with 100 mL of 0.6 M HCl and 100 mL of saturated $NaHCO_3$ solution, and then extracted with CH_2Cl_2 (100 mL × 3) and dried over $MgSO_4$. The solvent was removed by evaporation and the crude product was purified by flash chromatography (silica gel, gradient elution: petroleum ether/ethyl acetate 1 : 1 to 0 : 1) to give the monomer as a yellowish oil (4.33 g, yield: 68%). ^{1}H NMR (400 MHz, $CDCl_3$): δ = 1.87 (app qn, J = 6.6 Hz, 2H, C$^{\alpha}$***H*****$_2$** pyrrolidine), 1.97 (app qn, J = 6.6 Hz, 2H, C$^{\alpha}$***H*****$_2$** pyrrolidine), 3.54 (app qu, J = 6.2 Hz, 4H,

$C^{\beta}H_2$ pyrrolidine), 5.65 (dd, J = 9.9, 2.5 Hz, 1H, CH_2=CH–), 6.36 (dd, J = 16.7, 2.6 Hz, 1H, CH_2=CH–), 6.45 (dd, J = 16.8, 9.8 Hz, 1H, CH_2=CH–); ^{13}C NMR (101 MHz, $CDCl_3$): δ = 24.28 (CH_2–CH_2), 26.03 (CH_2–CH_2), 45.71 (CH_2–N–CH_2), 46.51 (CH_2–N–CH_2), 126.95 (CH_2–CH), 128.94 (CH_2–CH), 164.30 (C=O).

Synthesis of monomer *N*-acryloyl-L-proline (A-Pro-OH)

The polymerisable L-proline was synthesised following a reported procedure.[35] A stirred solution of L-proline (5 g, 43 mmol) in 2 M aqueous KOH (20 mL, 52 mmol) was cooled down to −78 °C (using an acetone-dry ice bath) and diluted with acetone (26 mL). Acryloyl chloride (4.34 g, 48 mmol) dissolved in acetone (26 mL) and 2 M aqueous KOH solution (30 mL, 61 mmol) were added dropwise over 40 min simultaneously to the previous proline solution, and then stirred at room temperature for 3 h. Acetone was removed by vacuum evaporation and the product was acidified using 2 M HCl (25 mL) while stirring the mixture. Then, the product was extracted with chloroform and washed with brine, dried with $MgSO_4$ and finally concentrated by vacuum evaporation. The residue was purified by recrystallisation with ethyl acetate to obtain the amide monomer as a white powder (4.9 g, 70% yield). ^{1}H NMR (400 MHz, DMSO-d_6): δ = 1.79–1.97 (m, 4H, –CH_2– pyrrolidine ring), 2.03–2.29 (m, 4H, –CH_2– pyrrolidine ring), 3.45 (m, 2H, –C$^{\beta}H_2$– pyrrolidine ring), 3.45 (m, 2H, –C$^{\beta}H_2$– pyrrolidine ring), 4.29 (dd, J = 8.8, 3.8 Hz, 1H, C$^{\alpha}H$ pyrrolidine ring), 4.64 (dd, J = 8.6, 2.8 Hz, 1H, C$^{\alpha}H$ proline), 3.62 (dd, J = 10.3, 2.5 Hz, 1H, CH_2=CH–), 5.71 (dd, J = 10.3, 2.2 Hz, 1H, CH_2=CH–), 6.12 (dd, J = 16.6, 2.4 Hz, 1H, CH_2=CH–), 6.14 (dd, J = 16.7, 2.3 Hz, CH_2=CH–), 6.36 (dd, J = 16.8, 10.4 Hz, 1H, CH_2=CH–), 6.62 (dd, J = 16.8, 10.3 Hz, 1H, CH_2=CH–), 12.59 (br s, 1H, –COOH). ^{13}C NMR (101 MHz, DMSO-d_6): δ = 22.61 (–CH_2– pyrrolidine ring), 24.82 (–CH_2– pyrrolidine ring), 29.18 (–CH_2– pyrrolidine ring), 31.20 (–CH_2– pyrrolidine ring), 46.57 (–CH_2– pyrrolidine ring), 47.03 (–CH_2– pyrrolidine ring), 59.01 (C^{α}H pyrrolidine ring), 127.25 (CH_2=CH–), 127.82 (CH_2=CH–), 129.70 (CH_2=CH–), 163.74 (–CO–CH–CH_2), 164.28 (–CO–CH–CH_2), 173.78 (–COOH), 174.19 (–COOH). The presence of two signals for each of the protons and most of the carbon atoms of A-Pro-OH suggests slow rotation (in the NMR time scale) around the amide bond.

Nanogels synthesis

Nanogels **N1–N25** were prepared by high dilution radical polymerisation following a previously reported procedure.[36] Thermoresponsive monomers (NIPAM, NPAM, and NAPr) and MBA (as a crosslinker, CL) in different monomer : CL ratios (see feeding composition in mol% monomer in Table 1 and the detailed composition in mmol in Table SI-1 of the ESI†) were dissolved in DMSO in a Wheaton bottle. The volume of solvent was adjusted to give a total monomer concentration (C_M) of 1%. Twice recrystallised AIBN as an initiator (1%) was then added to the solution. The Wheaton bottle was sealed and degassed through three vacuum/N_2 cycles. The reaction mixture was then heated to 70 °C for 48 h. The nanogel clear solution was dialysed (MWCO 3500 Da, diameter 22 mm) against deionised water for 3 days with frequent changes. The nanogel solution was frozen and lyophilised (Labconco FreeZone 6) to give white flakes. All the nanogel samples were stored at room temperature. Polymerisations for NMR analysis were performed following the same procedure using DMSO-d_6 as solvent. Using a microsyringe, 500 μL aliquots of starting and final reaction mixtures were transferred to NMR tubes. An appropriate volume of an internal standard stock solution (1,2,4,5-tetramethylbenzene in DMSO-d_6) was added to each tube and ^{1}H NMR spectra were recorded. The spectra acquired were phased and integrated identically using an automated procedure. The concentrations of the monomers and the crosslinker in the initial and final reaction mixtures were calculated by comparing the intensities of peaks at 5.55 ppm (NIPAM), 5.57 ppm (NPAM), 6.58 ppm (NAPr), 6.62 and 6.36 ppm (A-Pro-OH) and 4.56 or 5.63 ppm (MBA), and the peak of the internal standard at 6.9 ppm. The ^{1}H NMR spectra used to calculate monomer and overall conversions of polymerisation **N1** are shown in Fig. SI-1 of the ESI,† as a representative example of all ^{1}H NMR analyses. Calculated conversions for nanogels **N1–N25** are reported in Table 1 and Table SI-3 in the ESI.† Dual temperature and pH sensitive-based nanogels **N26–N31** were prepared as described previously here but using pH-responsive monomers A-Pro-OH or AAc, together with thermoresponsive monomer NPAM and/or NAPr, and MBA as CL in different ratios. Feeding compositions in mol% monomer are reported in Table 2 of this manuscript, and the detailed composition in mmol in Table SI-2 of the ESI.† Results of NMR analyses of polymerisations **N26–N30** are reported in Table SI-4 of the ESI.† Dye loaded nanogel **N30D** was prepared as nanogel **N30** with the addition of 2.5 mol% of Nile Blue A (NBA), using the same mol% as A-Pro-OH (see Table 2). The NBA loading was determined by dialysing (MWCO 3500 Da, length 5 cm) 1 mL of a nanogel **N30D** solution, after 48 h polymerisation, against water following the procedure described above. The non-loaded amount of NBA was quantified by measuring the absorbance of the collected supernatants by UV-Vis at 634 nm. The extinction coefficient of NBA in water at pH 7.4 (ε_{634} = 13 615 M^{-1} cm^{-1}) was previously determined from a calibration curve (Fig. SI-2 in the ESI†). The dye loading efficiency was calculated as the percentage ratio between the mass of the dye incorporated to the total mass of the dye uploaded to the nanogel. For the characterisation of nanogel **N30** at different pH values, a 1 mg mL^{-1} solution was prepared and the pH was adjusted using HCl (1 M) and NaOH (1 M) solutions in deionised water.

pH–Temperature release studies of Nile Blue A (NBA)

For the release studies, 1 mL of an aqueous solution of nanogel **N30D** (1 mg mL^{-1}) at pH 7.4, 6.5 or 5.2 was placed in a dialysis bag (MWCO 3500 Da, length 5 cm). The membrane was then immediately introduced into a vial with 20 mL of water at the corresponding pH and at room temperature. 1 mL aliquots of this aqueous solution containing the dye released by **N30D** were collected at 4, 10 and 24 hours. 1 mL of a fresh aqueous solution (at the specific pH) was added to the vials

after every aliquot collection to keep constant both the volume and pH. The experiments were repeated following the same procedure but keeping the solutions at 43 °C using a temperature-controlled oil bath. The released NBA from **N30D** was quantified with time at both temperatures by measuring the emission intensity (λ_{exc} = 634 nm, λ_{em} = 665 nm) of the aliquots collected.

Results and discussion

Thermoresponsive nanogels

We initially focused on the development of a library of crosslinked nanogels using three different thermoresponsive monomers and different concentrations of crosslinkers. The characterisation of these nanogels allowed us to evaluate how the chemical composition could impact their morphology and thermoresponsive properties.

The structures of the monomers and the crosslinker used are shown in Fig. 1. The monomers were reacted with *N*,*N*′-methylenebisacrylamide (MBA) as a crosslinker, using high dilution radical polymerisation,[36] which allows formation of nano-sized particles without the use of surfactants. The thermoresponsive monomers used are *N*-isopropylacrylamide (NIPAM), *N*-*n*-propylacrylamide (NPAM) and *N*-*n*-acryloylpyrrolidine (NAPr), all of which are known to form linear polymers with different values of lower critical solution temperature (LCST), *i.e.* 32 °C for NIPAM,[37] 22–24 °C for NPAM[38] and 50 °C for NAPr.[39] NIPAM is one of the most frequently used monomers for the preparation of thermoresponsive polymers and was used in this work as the reference monomer. NPAM, the linear isomer of NIPAM, was selected on the basis that it could increase the overall hydrophobicity of the nanogels while keeping a similar monomer structure. Finally, NAPr with a tertiary amide and higher LCST (50 °C) was expected to increase the overall hydrophilicity of the polymer. There is limited consistency in the literature on the use of the terms hydrophobicity or hydrophilicity when referring to polymers.[40] Therefore, in the context of this work, we decided to use the more general term "degree of hydrophilicity".

Five sets of polymers based on NIPAM (**N1–N5**), NPAM (**N6–N10**), NAPr (**N11–N15**), or combinations of NIPAM-NAPr (**N16–N20**) and NPAM-NAPr (**N21–N25**) were synthesised with percentages of the crosslinker MBA ranging between 10% and 50%. The detailed compositions of all the preparations are presented in Tables 1 and SI-1 (ESI†). The incorporation of monomers into the nanogels was confirmed by FT-IR (see spectra of **N1**, **N6** and **N11** in Fig. SI-3–SI-7 of the ESI,† as representative examples for all nanogels). Conversions for all the polymerisations were calculated by ^{1}H NMR and the results are reported in Table 1 (overall conversions, *C*) and Table SI-3† (individual monomer conversions). These data indicate that the chemical structure of the monomers impacts the overall conversion, with individual values suggesting that NAPr is incorporated at a similar rate as the crosslinker MBA, with >90% conversion after 48 h. NIPAM and NPAM showed similar behaviour, both displaying incorporation rates lower than MBA. The slower incorporation of NIPAM and NPAM results in lower overall conversions, in particular for those formulations containing lower percentages of crosslinker. This means that unreacted monomers are still present in the final polymerisation mixtures and subsequently lost during the isolation step. This is further confirmed by the chemical yields obtained, which are particularly low for **N1**, **N2** and **N6** and **N7**.

Table 1 Chemical compositions and yields of nanogels **N1–N25**

Nanogel No.	NIPAM	NPAM	NAPr	MBA	C^a	Y^b
	mol% monomer			mol% CL	%	%
N1	90	0	0	10	65.4	43.7
N2	80	0	0	20	72.4	49.6
N3	70	0	0	30	82.2	56.2
N4	60	0	0	40	86.7	87.1
N5	50	0	0	50	85.1	92.4
N6	0	90	0	10	61.7	42.2
N7	0	80	0	20	66.9	49.6
N8	0	70	0	30	71.4	51.1
N9	0	60	0	40	80.5	82.2
N10	0	50	0	50	82.4	82.8
N11	0	0	90	10	96.2	80.4
N12	0	0	80	20	96.2	78.7
N13	0	0	70	30	97.5	71.9
N14	0	0	60	40	97.2	93.2
N15	0	0	50	50	98.1	95.6
N16	40	0	50	10	89.1	56.8
N17	40	0	40	20	90.3	81.3
N18	40	0	30	30	89.4	62.3
N19	40	0	20	40	84.0	79.4
N20	40	0	10	50	88.3	51.3
N21	0	40	50	10	86.5	65.1
N22	0	40	40	20	85.3	68.1
N23	0	40	30	30	87.2	61.1
N24	0	40	20	40	88.9	63.1
N25	0	40	10	50	86.7	55.8

^{a} *C* is the overall conversion calculated using NMR. ^{b} *Y* is the nanogel isolated yield.

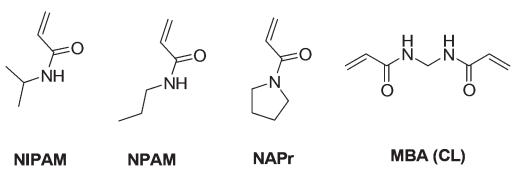

Fig. 1 The thermoresponsive monomers (NIPAM, NPAM and NAPr) and the crosslinker (MBA) used in the preparation of nanogels **N1–N25**.

The hydrodynamic diameter (d_h) for nanogels **N1–N25** was obtained *via* measurements of dynamic light scattering and was found to be less than 50 nm in all cases. As illustrated in Fig. 2a, the data suggest a clear trend of the particle size increasing with the crosslinker content in all nanogel sets, coupled with a decrease in polydispersity. This observation is consistent with the data reported by Pelton *et al.*[41] and by Varga *et al.*[42] for NIPAM-based MBA crosslinked microgels,

and the data recently reported by our group for NIPAM-based MBA crosslinked nanogels.[43] The change in chemical composition results in the variation of the particle surface, which will impact its solvation and affect its diffusion speed, resulting in apparent changes in size.[44] Furthermore, the increase in crosslinker content, leading to a more rigid structure, also affects polymer conformation and its potential to be assimilated into a sphere. Interestingly, the small differences in the chemical structure of the thermoresponsive monomers used do not appear to have a significant impact on the particle size of the isolated nanogels.

The thermoresponsive behaviour of the 25 nanogels was probed by determining their VPTT values, presented in Fig. 2b as a function of CL content for each nanogel series. The VPTT for each nanogel was obtained by UV-Vis spectroscopy, from the inflection point in the transmittance *vs.* temperature data (Fig. SI-40 and SI-41 in the ESI†). For a small number of nanogels (**N9**, **N10** and **N25**) the VPTT could not be determined as the transition probably occurs outside the range of temperatures evaluated (20–80 °C). The thermoresponsive properties of the nanogels could also be easily observed by the naked eye (inset to Fig. 2b) as the appearance of the nanogels in aqueous solution changes above VPTT, from transparent to cloudy solution. This effect is attributed to the disruption of hydrogen bonds between the –NH groups and H_2O molecules, concomitant with the polymer conformational changes occurring at the VPTT.

Similar behaviour is observed for all thermoresponsive nanogels (Fig. 2b). The introduction of the crosslinker, even at low concentration (10%), leads to increased rigidity, which results in higher VPTT values, compared to the linear forms. As the crosslinker content increases above 20%–30%, the rigidity of the matrix no longer allows conformational changes, resulting in a significant decrease in VPTT values and thus loss of the thermoresponsive properties. However, at lower crosslinker content, the hydrophilicity of the thermoresponsive monomers has an influence on VPTT. Comparison of data at 10% MBA content shows VPTT rising from NPAM (**N6**, 33.5 °C) to NIPAM (**N1**, 40.0 °C) to NAPr (**N11**, 55.0 °C), following the same trend observed for the LCSTs. It is noteworthy that in the case of NIPAM and NPAM when going from 10 to 20% MBA, a slight increase in VPTT is observed. This is consistent with the results reported on the dual nature of NIPAM-based polymers by Pelton,[40] who highlighted the presence of both hydrophilic and hydrophobic domains in PNIPAM to explain its behaviour above LCST.

Cooperative effects were expected from the combination of two monomers in nanogels **N16–N25**, as observed by Kono *et al.*[34] for NAPr-NIPAM polymer-modified liposomes. In particular, by fixing the content of NIPAM and NPAM at 40%, and varying the content of NAPr, we investigated the effect of the latter on the overall degree of hydrophilicity of the nanogels. Strikingly, the NIPAM-modified series (**N16–N20**) showed lower VPTT values than the NPAM series (**N21–N25**), contrary to the trend in LCSTs. Two factors can contribute to this result. On the one hand, the two sets of nanogels have different particle sizes, especially at CL < 30% (see Fig. 2a); on the other hand, the significant difference in VPTT at 20% crosslinker suggests that the degree of hydrophilicity of the nanogels is considerably different. This may be justified by the assumption that NIPAM and NPAM, due to their varied degrees of hydrophilicity, combine in different ways with NAPr and MBA during polymerisation, resulting in polymer matrices with very different architectures.[45,46] Finally, the stability and thermoresponse reversibility of these colloidal systems were investigated. Heating and cooling cycles confirmed a reversible behaviour for **N1**, **N6** and **N11** (Fig. SI-42 in the ESI†), which after 6 cycles showed no loss of thermoresponsive characteristics.

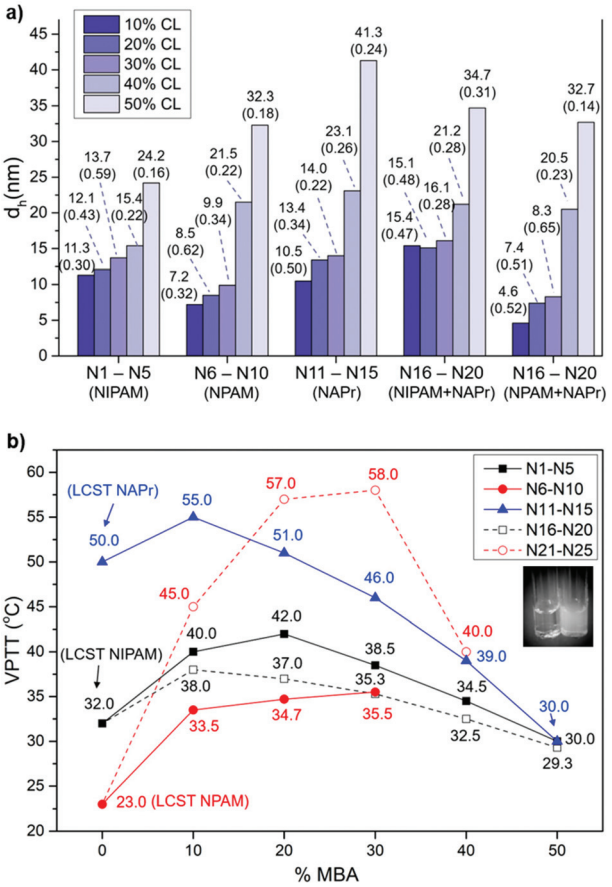

Fig. 2 (a) Graph showing the impact of chemical composition on particle size for nanogels **N1–N25**. d_h is the nanogel hydrodynamic diameter *via* volume. The polydispersity index (PdI) measured by DLS is indicated in brackets below each d_h value. See the original raw DLS data in the ESI (Fig. SI-8–SI-33†). (b) VPTT of nanogel series **N1–N5** (NIPAM), **N6–N10** (NPAM), **N11–N15** (NAPr), **N16–N20** (NIPAM + NAPr) and **N21–N25** (NPAM + NAPr) presented as a function of percentage of the crosslinker (MBA). LCST values for linear polymers of NIPAM, NPAM and NAPr are included in the graph for reference. VPTT values were measured at a concentration of 1 mg mL^{-1}. Full profiles of the transmittance (%) change with temperature are included in the ESI (Fig. SI-40 and SI-41†). No transition was observed for nanogels **N9**, **N10** and **N25**. Inset: Photographs of a solution of polymer **N1** below (left) the VPTT and the collapsed state (right) above the VPTT.

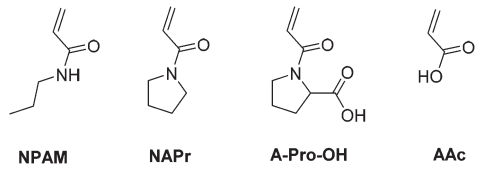

Fig. 3 Thermoresponsive monomers (NPAM and NAPr) and pH-responsive monomers (A-Pro-OH and AAc) used in the preparation of nanogels **N26–N31**.

Dual pH–temperature responsive nanogels

The results discussed in the previous section demonstrate that the choice of thermoresponsive monomer and crosslinker content allows fine-tuning the degree of hydrophilicity and thermoresponsive properties of the nanogels. As mentioned previously, systems with dual stimuli are potentially very interesting.[15] In the design of dual smart materials, acidic pH responsive polymers have been well exploited, for example, by incorporating acrylic acid, methacrylic acid, undecanoic acid or maleic acid as monomers.[29–32,47,48] Despite their efficiency, these systems have limitations in terms of biocompatibility[49] or thermoresponsive control. In this work, we introduced a pH switch as a second stimulus for the thermoresponsive nanogels. We used a co-monomer based on the chemical structure of NAPr with an additional –COOH moiety. The carboxylic acid brings the benefits of drug controlled release through ionic interactions with cationic drugs at neutral pH, and release at pathological acidic environments. Thus, a polymerisable unit, based on the amino acid L-proline (A-Pro-OH, shown in Fig. 3), was identified as a potential pH responsive switch.

(NPAM : MBA 90 : 10 VPTT *ca.* 34 °C) was selected as the most suitable one.

Five nanogels, **N26–N30**, with varying percentages of monomer A-Pro-OH and NPAM and a constant 10 mol% of MBA were prepared and characterised. In order to explore the relationship between different co-monomers, acrylic acid (AAc) and NAPr were polymerised together in preparation **N31** as a control.[52] The use of acrylic acid to introduce a pH switch has been widely reported.[53] The monomer : CL feed composition of these new nanogels is detailed in Table 2 (and Table SI-2 in the ESI†). Overall conversion values calculated by NMR for polymers **N26–N30** range between 65% and 75% (Table SI-4†). These values are slightly lower than those obtained for the **N1–N25** series; however, for consistency with the previous experiments, the polymerisation parameters were not altered. The chemical yields of the isolated nanogels are also lower due to the loss of short chains during purification. Conversion values for A-Pro-OH suggest a lower degree of incorporation than that for NAPr but higher than those observed for NIPAM or NPAM in nanogels **N1–N25**.

The introduction of A-Pro-OH in concentrations ≥5% in the NPAM-based nanogels results in an apparent increase in particle size, as determined by DLS (Table 2 and Fig. SI-33–SI-39†). This can be attributed to a significant increase in the degree of swelling of the nanogels in water, which increases the solvation sphere. When the concentration of A-Pro-OH is 2.5% in nanogel **N30**, this effect is not so significant and the particle size is comparable to nanogel **N6**. Particle size was measured by two different techniques for **N6** and **N30** (Fig. SI-43 in the ESI†): DLS (7.2 nm and 4.3 nm for **N6** and **N30**, respectively) and TEM (5.7 nm and 3.2 nm, respectively). Both techniques afforded similar sizes, thus suggesting that

Table 2 Chemical composition and characterisation data for nanogels **N26–N31**

Nanogel No.	NPAM	A-Pr-OH	NAPr	AAc	MBA	Y^a	d_h [b,e]	ζ [d,e]	VPTT[e]
	mol% monomer				mol% CL	%	nm (PdI)[c]	mV	°C
N26	70	20	0	0	10	74.3	102.4 (0.26)	−36.0 ± 2.9	NT
N27	75	15	0	0	10	60.4	123.2 (0.20)	−28.7 ± 6.3	NT
N28	80	10	0	0	10	54.5	111.0 (0.33)	−25.9 ± 3.9	62.0
N29	85	5	0	0	10	46.1	116.1 (0.29)	−25.1 ± 2.6	54.5
N30	87.5	2.5	0	0	10	43.0	4.3 (0.19)	−19.2 ± 7.6	43.0
N31	85	0	2.5	2.5	10	45.1	5.8 (0.39)	−22.2 ± 0.3	37.5
N30D	87.5	2.5	0	0	10	44.3	4.7 (0.36)	−23.6 ± 1.1	42.5

[a] Y is nanogel polymerisation yield. [b] d_h is nanogel hydrodynamic diameter *via* volume. [c] PdI is the polydispersity index. [d] ζ is the zetapotential measured by DLS. [e] Measured at a concentration of 1 mg mL^{-1} in deionised water (pH was not adjusted). NT stands for no transition.

Studies have shown that the introduction of hydrophilic co-monomers can result in an increase of VPTT.[50,51] A-Pro-OH having a carboxylic acid group is more hydrophilic than any of the monomers previously used in our work (NIPAM, NPAM or NAPr). It was decided to introduce the pH switch in the NPAM-based nanogels as they displayed the lowest VPTTs (Fig. 2b). The goal was to obtain nanogels with a transition temperature close to physiological values. For this reason nanogel **N6** the addition of a second functionality in **N30** (pH-switch) at 2.5% concentration does not impact particle size. The small differences observed can be explained by the nature of the two techniques: DLS measurements provide a solvated hydrodynamic size of the gel nanoparticles, whereas in TEM the gel nanoparticles are deposited on a solid support and measured in the dry state. Additionally, TEM images confirm the approximately spherical appearance of the nanogels. Finally, small

particles were also observed for the control nanogel **N31** (5.8 nm measured by DLS) containing the combination of NAPr and AAc instead of A-Pro-OH.

The zeta potential of nanogels **N26–31** was also measured by DLS and a negative surface charge was determined for all of them (Table 2 and Fig. SI-44–SI-50 in the ESI†). In particular, for the nanogels prepared with different ratios of A-Pro-OH/NPAM monomers and crosslinked with 10 mol% of MBA (**N26–N30**), a direct correlation between the percentage of A-Pro-OH and charge was observed. Nanogels **N30** and **N31**, incorporating different monomers (A-Pr-OH in **N30** and NAPr/AAc in **N31**),[52] showed similar zeta potential data (−19.2 and −22.2 mV, respectively). This confirms that the introduction of NAPr does not impact the gel nanoparticle surface charge and hence this can be attributed only to the presence of AAc or A-Pro-OH monomers with carboxylic acid functionalities.

The VPTT values of nanogels **N26–N31** were obtained to evaluate the influence of the pH switch on thermoresponsive properties. The VPTT data (Table 2 and Fig. SI-50†) suggest a maximum limit of 5% of A-Pro-OH required to maintain thermoresponsiveness, while higher concentrations do not lead to a clear data profile. This can be attributed to changes in the degree of hydrophilicity. The use of NPAM lowers the responsiveness (as demonstrated previously) while the use of A-Pro-OH as co-monomer increases the overall degree of hydrophilicity and thus also the VPTT. The VPTT values determined for nanogels **N30** (based on monomers NPAM and A-Pro-OH) and **N31** (based on monomers NPAM, AAc and NAPr)[52] differ by 5 °C (43 °C *versus* 37.5 °C). This difference is likely to be due to variations in the chemical structures of the monomers used. The higher VPTT for nanogel **N30** can be considered an advantage for future biomed applications, especially in areas of drug release such as pathological environments which typically present higher temperatures than healthy tissues (heated cancer tissues present temperatures around 42 °C).[54] Therefore, nanogel **N30** was identified as the material with the best characteristics as a drug delivery vehicle and selected for further evaluation.

The behaviour of polymer **N30** at different pH values was evaluated and compared with **N6** (nanogel without a carboxylic acid moiety). UV-Vis studies demonstrated the possibility of modulating the VPTT of nanogel **N30** by changing the pH: 43 °C at pH 7.4, and 41.5 °C at pH 5.2, while the VPTT for **N6** remained unaltered with pH (Fig. 4). This directly confirms the pH responsive nature of nanogel **N30**. The particle size for **N30** was also studied as a function of pH and temperature (Fig. 5). As expected, at the three different pH values examined (7.4, 6.5 and 5.5), the size of the particles measured is larger as they aggregate at temperatures above the VPTT. Furthermore, zeta potential measurements for **N30** (Fig. SI-53–SI-55 in the ESI†) confirm a decrease in nanoparticle surface charge upon increasing the degree of protonation at lower pH (−22.2 mV at pH 7.4, −12.9 mV at pH 6.5 and −7.4 at pH 5.2). Thus, all the characterisation data suggest that NPAM-based nanogels incorporating A-Pro-OH monomer, and in particular preparation

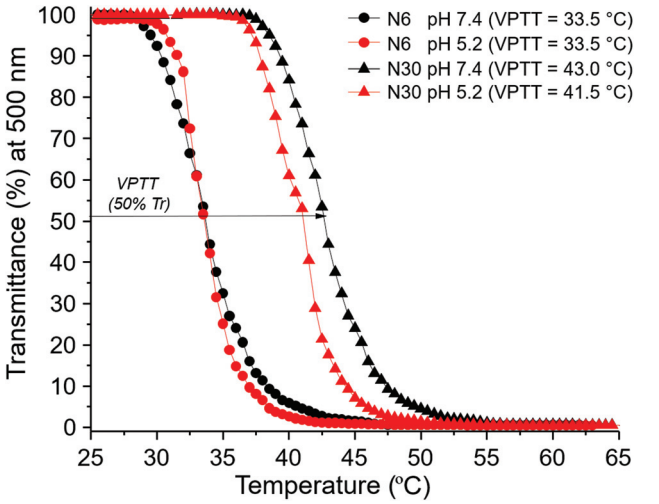

Fig. 4 Transmittance change with increasing temperature for nanogels **N6** and **N30** at two different pH values (5.2 and 7.4). Transmittance was measured at 500 nm and at a polymer concentration of 1 mg mL^{-1}.

N30, offer a valid alternative to the more traditional and less versatile AAc based materials.

Drug release application

Nile Blue A (NBA)[55,56] was chosen as a model-drug to evaluate the dual-stimuli nanogel **N30** as a drug delivery vehicle. This molecule presents both low molecular weight and cationic charge, which allows an ionic interaction with the carboxylic groups of the A-Pro-OH monomer. In our case, the dye was entrapped in the inner cavities of the 3D nanogel network during the polymerisation step. This favours the interactions between the organic matrix and the model drug, and maximises the loading. The composition of the drug loaded nanogel **N30D** is shown in Table 2, along with the characterisation data. The loading efficiency was calculated using UV-Vis spectroscopy as the percentage ratio between the mass of dye incorporated to the total mass of drug used to upload the nanogel. The loading efficiency was found to be 37%, a value that is consistent with previously reported data.[57]

The stimuli-responsive drug release of nanogel **N30D** was probed by monitoring the fluorescence emission of NBA upon release,[58] benefiting from the unique emission of this species at 665 nm (λ_{ex} 634 nm). The release of NBA was measured at different time intervals (4 h, 10 h and 24 h), at three different pHs (7.4, 6.5 and 5.2) and at two temperatures (23 °C and 43 °C, the VPTT of **N30D**). The combined data are presented in Fig. 6. The lowest release is observed at pH 7.4 and 23 °C, as expected, confirming that the electrostatic interactions between the dye and the monomer are stable under those conditions. The slight increase observed at higher temperature, at 24 h, is likely to be the result of shrinkage of the polymeric matrix as the temperature reaches VPTT. The same temperature effect is observed at all pH values, confirming the thermoresponsive nature of the polymer and the role of temperature

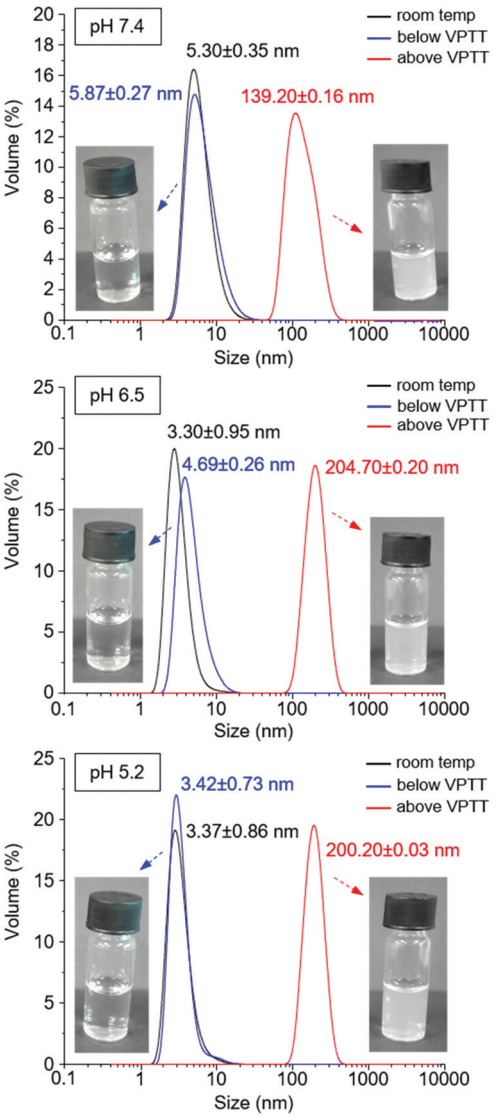

Fig. 5 Hydrodynamic diameter by volume for **N30** as a function of temperature at pH 7.4, 6.5 and 5.2 (concentration = 1 mg mL^{-1}). Insets show photographs of the nanogels in water below and above VPTT at each of the different pH values.

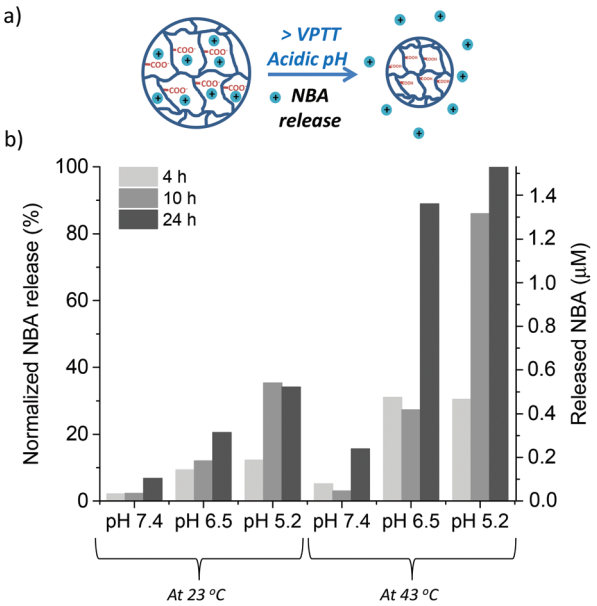

Fig. 6 (a) Schematic representation of the mechanism of drug release under acidic conditions and above VPTT following protonation of the carboxylic acid moieties of the L-proline based co-monomer. (b) Cargo (NBA) release from nanogel **N30D** as a function of time in aqueous solutions at different pH values, at 23 °C and 43 °C (above VPTT), respectively.

in controlling the release of the drug. The highest release occurred at the lowest pH (5.2) and higher temperature (43 °C); these results are justified by two factors: (i) the more acidic conditions (pH 5.2) lead to a significant disruption of the NBA-COOH interactions, resulting in eight times more dye released that at neutral pH 7.4; (ii) the shrinkage of the polymer above its VPTT pushes out the water and the NBA molecules, contributing to higher dye release over time.

The data reported demonstrate the dual stimuli responsive properties of nanogel **N30D**, which are dependent on both pH and temperature. Additionally, the small library of nanogels developed in this work show the feasibility of fine tuning the thermoresponsive properties of nanogels, in combination with specific pH-triggered release. This type of carriers would be potentially useful in applications such as cancer therapy, where the lower pH of the tumour cell, together with higher localised heat, would favour drug release and minimise side effects. Some liposomes formulations have been already developed for drug delivery at temperatures close to hyperthermia (40–45 °C).[59] Furthermore, the electrostatic interactions between the positive charged NBA, acting as drug model, and the negatively charged L-proline units within nanogel **N30D** are maintained at pH 7.4 over a 24 h period, while at lower pH the release occurs. Thus, these nanogels could also be useful for future *in vitro* studies in cancer cells.[60] In the literature, the higher affinity of NBA for cancer cells *vs.* healthy ones[61] has been reported, making this molecule a perfect candidate for such studies. Finally, nanogel **N30D** can potentially be used for delivery of other low molecular weight and positively charged anti-cancer drug molecules, such as Paclitaxel or Adriamycin. These molecules have been shown to be released at pHs below 6.5, typical of tumour cell environments.[62]

Conclusions

A library of 25 nanogel formulations was developed using three different thermoresponsive monomers, NIPAM, NPAM and NAPr, *via* high dilution free radical polymerisation and crosslinked by MBA. Detailed characterisation of particle size and VPTT showed that the choice of monomers and crosslinker content allows tailoring the final degree of hydrophilicity, size and thermoresponsive properties of the nanogel "on

demand", depending on the application. Nanogel **N6**, prepared with the most hydrophobic monomer NPAM and MBA, in a 90 : 10 ratio, displayed a VPTT of 33.5 °C, considered to be suitable as a basis for further modifications. A dual pH–temperature responsive nanogel was obtained by the addition of a proline-based monomer (A-Pro-OH) to the **N6** formulation. The NPAM nanogel containing 10 mol% MBA and 2.5 mol% of A-Pro-OH was then used as a drug delivery vehicle to probe the dual pH–temperature stimuli and demonstrate tailored drug release. Nile Blue A, used as a cationic model drug, was uploaded into the nanogel exploiting electrostatic interactions. The data clearly demonstrate a tailored delivery controlled by both temperature and pH, with the highest release observed after 24 h at pH 5.2 and temperatures above 42 °C. These results suggest that this type of nanogel may be a promising tool for future applications in targeted drug release, especially in cancer tissues and for the treatment of inflammatory conditions.

Conflicts of interest

There are no conflicts to declare.

Acknowledgements

This work was supported by the European Commission *via* the ITN NANODRUG (Marie Curie Actions GA no. 289454, YS and AMC).

Notes and references

1 S. Mura, J. Nicolas and P. Couvreur, *Nat. Mater.*, 2013, **12**, 991–1003.
2 A. A. Moghanjoughi, D. Khoshnevis and A. Zarrabi, *Drug Delivery Transl. Res.*, 2016, **6**, 333–340.
3 A. C. Hunter and S. M. Moghimi, *Polym. Chem.*, 2017, **8**, 41–51.
4 P. L. Ritger and N. A. Peppas, *J. Controlled Release*, 1987, **5**, 23–36.
5 J. Liu, Y. Huang, A. Kumar, A. Tan, S. Jin, A. Mozhi and X.-J. Liang, *Biotechnol. Adv.*, 2014, **32**, 693–710.
6 I. Berndt, C. Popescu, F. J. Wortmann and W. Richtering, *Angew. Chem.*, 2006, **45**, 1081–1085.
7 F. Ercole, T. P. Davis and R. A. Evans, *Polym. Chem.*, 2010, **1**, 37–54.
8 V. V. Mody, A. Cox, S. Shah, A. Singh, W. Bevins and H. Parihar, *Appl. Nanosci.*, 2014, **4**, 385–392.
9 C. Konak, J. Panek and M. Hrubý, *Colloid Polym. Sci.*, 2007, **285**, 1433–1439.
10 M. B. Yatvin, J. N. Weinstein, W. H. Dennis and R. Blumenthal, *Science*, 1978, **202**, 1290–1293.
11 S. Ganta, H. Devalapally, A. Shahiwala and M. Amiji, *J. Controlled Release*, 2008, **126**, 187–204.
12 M. A. Ward and T. K. Georgiou, *Polymer*, 2011, **3**, 1215–1242.
13 H. Tekin, J. G. Sanchez, T. Tsinman, R. Langer and A. Khademhosseini, *AIChE J.*, 2011, **12**, 3249–3258.
14 J. V. Ray, F. Mirata, C. Perollier, M. Arotcarena, S. Bayoudth and M. Resmini, *Anal. Bioanal. Chem.*, 2016, **408**, 1855–1861.
15 J. Zhuang, M. R. Gordon, J. Ventura, L. Li and S. Thayumanavan, *Chem. Soc. Rev.*, 2013, **42**, 7421–7435.
16 D. Chen, H. Yu, K. Sun, W. Liu and H. Wang, *Drug Delivery*, 2014, **4**, 258–264.
17 R. Cheng, F. Meng, C. Deng, H. A. Klok and Z. Zhong, *Biomaterials*, 2013, **34**, 3647–3657.
18 D. Schmaljohann, *Adv. Drug Delivery Rev.*, 2006, **58**, 1655–1670.
19 H. Chea and J. C. M. van Hest, *J. Mater. Chem. B*, 2016, **4**, 4632–4647.
20 V. Brunetti, L. M. Boucheta and M. C. Strumia, *Nanoscale*, 2015, **7**, 3808–3816.
21 S. Merino, C. Martin, K. Kostarelos, M. Prato and E. Vazquez, *ACS Nano*, 2015, **9**, 4686–4697.
22 M. Molina, M. Asadian-Birjand, J. Balach, J. Bergueiro, E. Miceli and M. Calderón, *Chem. Soc. Rev.*, 2015, **44**, 6161–6186.
23 H. Staudinger and E. Husemann, *Ber. Dtsch. Chem. Ges.*, 1935, **68**, 1618–1634.
24 S. A. Papadimitriou, M. P. Robin, D. Ceric, R. K. O'Reilly, S. Marino and M. Resmini, *Nanoscale*, 2016, **8**, 17340.
25 R. T. Chacko, J. Ventura, J. Zhuang and S. Thayumanava, *Adv. Drug Delivery Rev.*, 2012, **64**, 836–851.
26 Y. Guan and Y. Zhang, *Soft Matter*, 2011, **7**, 6375–6384.
27 L. A. Lyon, Z. Meng, N. Singh, C. D. Sorrell and A. St. John, *Chem. Soc. Rev.*, 2009, **38**, 865–874.
28 R. Pelton, *Adv. Colloid Interface Sci.*, 2000, **85**, 1–33.
29 S. Zhou and B. Chu, *J. Phys. Chem. B*, 1998, **102**, 1364–1371.
30 W. Xue, S. Champ and M. B. Higlin, *Polymer*, 2000, **41**, 7575–7581.
31 K. Liu, H. Guo and L. Zha, *Polym. Int.*, 2012, **61**, 1144–1150.
32 W. Xiong, W. Wang, Y. Wang, Y. Zhao, H. Chen, H. Xu and X. Yang, *Colloids Surf., B*, 2011, **84**, 447–453.
33 Y. Matsumaru, A. Hyodo, T. Nose, S. Ito, T. Hirano and S. Ohashi, *J. Biomater. Sci., Polym. Ed.*, 1996, **7**, 795–804.
34 K. Kono, R. Nakai, K. Morimoto and T. Takagishi, *Biochim. Biophys. Acta*, 1999, **1416**, 239–250.
35 H. Mori, I. Kato, M. Matsuyama and T. Endo, *Macromolecules*, 2008, **41**, 5604–5615.
36 S. C. Maddok, P. Pasetto and M. Resmini, *Chem. Commun.*, 2004, 536–537.
37 Y. Guan and Y. Zhang, *Soft Matter*, 2011, **7**, 6375–6384.
38 S. Y. Park, J. H. Yang, S. H. Yuk and M. S. John, *J. Polym. Sci., Part B: Polym. Phys.*, 1999, **37**, 1407–1411.
39 M. Abdul Haq, Y. Su and D. Wang, *Mater. Sci. Eng., C*, 2017, **70**, 842–855.
40 R. Pelton, *J. Colloid Interface Sci.*, 2010, **348**, 673–674.
41 J. Zhang and R. Pelton, *Langmuir*, 1999, **15**, 8032–8036.

42 I. Varga, T. Gilányi, R. Mészáros, G. Filipcsei and M. Zrínyi, *J. Phys. Chem. B*, 2001, **105**, 9071–9076.
43 K. Zielinska, H. Sun, R. A. Campbell, A. Zarbakhsh and M. Resmini, *Nanoscale*, 2016, **8**, 4951–4960.
44 http://149.171.168.221/partcat/wp-content/uploads/Malvern-Zetasizer-LS.pdf (accessed February 2018).
45 L. D. Taylor and L. D. Cerankowski, *J. Polym. Sci., Polym. Chem. Ed.*, 1975, **13**, 2551–2570.
46 Y. Xu, Y. Li, X. Cao, Q. Chen and Z. An, *Polym. Chem.*, 2014, **5**, 6244–6255.
47 A. C. Foss, T. Goto, M. Morishita and N. A. Peppas, *Eur. J. Pharm. Biopharm.*, 2004, **57**, 163–169.
48 C. Alvarez-Lorenzo and A. Concheiro, *J. Controlled Release*, 2002, **80**, 247–257.
49 K. Y. Lee and D. J. Mooney, *Chem. Rev.*, 2001, **101**, 1869–1879.
50 Y. H. Bae, T. Okano and S. W. Kim, *J. Polym. Sci., Part B: Polym. Phys.*, 1990, **28**, 923–936.
51 H. Mori, I. Kato and T. Endo, *Macromolecules*, 2009, **42**, 4985–4992.
52 K. Kratz, T. Hellweg and W. Eimer, *Colloids Surf., A*, 2000, **170**, 137–149.
53 M. J. Snowden, B. Z. Chowdhry, B. Vincent and G. E. Morris, *J. Chem. Soc., Faraday Trans.*, 1996, **92**, 5013–5016.
54 W. Xiong, W. Wang, Y. Wang, Y. Zhao, H. Chen, H. Xu and X. Yang, *Colloids Surf., B*, 2011, **84**, 447–453.
55 J. Jose and K. Burgess, *Tetrahedron*, 2006, **62**, 11021–11037.
56 C. Zhang, K. Zhao, T. Hu, X. Cui, N. Brown and T. Boland, *J. Controlled Release*, 2008, **131**, 128–136.
57 J. O. Kim, H. S. Oberoi, S. Desale, A. V. Kabanov and T. K. Bronich, *Polymer*, 2013, **21**, 981–993.
58 N. Kalva, N. Parekh and A. V. Ambade, *Polym. Chem.*, 2015, **6**, 6826–6835.
59 T. Tagami, W. D. Foltz, M. J. Ernsting, C. M. Lee, I. F. Tannock, J. P. May and S. D. Li, *Biomaterials*, 2011, **32**, 6570–6578.
60 C.-W. Lin, J. R. Shulok, S. D. Kirley, L. Cincotta and J. W. Foley, *Cancer Res.*, 1991, **51**, 2710–2719.
61 D. C. Nikas, J. W. Foley and P. M. Black, *Lasers Surg. Med.*, 2001, **29**, 11–17.
62 K. Engin, D. B. Leeper, J. R. Cater, A. J. Thistlethwaite, L. Tupchong and J. D. McFarlane, *Int. J. Hyperthermia*, 1995, **11**, 211–216.